Contribution of Loops and Nicks to the Formation of DNA Dumbbells: Melting Behavior and Ligand Binding†

Dionisios Rentzeperis, James Ho, and Luis A. Marky*

Department of Chemistry, New York University, New York, New York 10003

Received September 10, 1992; Revised Manuscript Received December 22, 1992

ABSTRACT: We have evaluated the thermodynamic contribution of thymine loops and nicks to the overall stability of double-helical DNA by investigating (1) the melting behavior of two unligated DNA dumbbells and their corresponding core duplexes and (2) the association of netropsin to the central core of four A·T base pairs of these molecules. Temperature-dependent UV absorption and differential scanning calorimetry techniques have been used to characterize the helix–coil transitions of all four deoxyoligonucleotide duplexes. In 10 mM NaP_i buffer at pH 7.0, all transitions were monophasic. The dumbbells melt with transition temperatures, T_m, independent of strand concentration, while each duplex melts with transition temperature dependence on strand concentration, characteristic of mono- and bimolecular processes, respectively. The T_m's for the dumbbells correspond to those of single hairpins containing only four base pairs in the stem. We obtain $dT_m/d \log [Na^+]$ values of 10.9–12.5 °C for these molecules, which correspond to similar counterion releases and suggest helical structures with similar charge densities and helical strandedness. Standard thermodynamics profiles at 5 °C reveal that the favorable free energy of forming these ordered structures results from the partial compensation of favorable enthalpies with unfavorable entropies. The stabilization of the dumbbells relative to the core duplexes is enthalpic, due to extra stacking of the nearest loop thymines on the G·C base pairs at both ends of the stem. The association of netropsin was used to thermodynamically probe the integrity of the base-pair stacking at the nick point in the center of the dumbbell molecules, GAT^TAC/GTAATC and CAT^TAG/CTAATG, by direct comparison with the similar sequences of the core duplexes without the nicks, GATTAC/GTAATC and CATTAG/CTAATG. In 10 mM NaP_i buffer at pH 7.0, netropsin binds to the central core of A·T base pairs of these four sequences with similar binding affinities of $\sim 10^8$ and similar thermodynamic profiles: $\Delta G°_b = -10.8$ kcal·mol^{-1}, $\Delta H°_b = -10.6$ kcal·mol^{-1}, and $T\Delta S°_b = +0.2$ kcal·mol^{-1}, with binding enthalpies independent of salt concentration. Therefore, all four sequences constitute similar binding sites for netropsin. However, we obtained $d \ln K_b/d \ln [Na^+]$ values of -1.0 for the dumbbells and -1.1 for the duplexes, consistent with the lower charge density of these helical structures. The difference of 0.1 is attributed to the absence of a phosphate group at the nick point. In the dumbbells, the presence of the loops creates additional sites for netropsin, formed by two G·C pairs at each end of duplex and the constrained loop groups (forming additional stacked base pairs in a double helical geometry), with binding affinities of $\sim 10^5$ and $\Delta H°_b$ of -5.1 kcal·mol^{-1}. Both parameters are dependent on salt concentration. Our combined results show that the presence of a nick in the center of the dumbbells is not affecting the overall stacking of the T^T/AA base pair at the center of the dumbbells but interrupts the cooperative melting of the whole molecule.

Hairpin structures are a common feature of RNA molecules (Uhlenbeck, 1987; Chastain & Tinoco, 1991; Hans & Pardi, 1991; Varani & Tinoco; 1991; Draper, 1992). Their presence in DNA molecules has been postulated to exist in regions of DNA containing palindromic sequences, which have been implicated to be involved in gene regulation (Maniatis et al., 1975; Muller & Fitch, 1982; Rosenberg & Court, 1979; Wells et al., 1980). Our current understanding of the structures and stability of DNA and RNA has been enhanced by thermodynamic investigations of the helix–coil transitions of model compounds such as those of oligonucleotides of known sequence (Gralla & Crothers, 1973; Uhlenbeck et al., 1973, Breslauer et al., 1986; Freier et al., 1986; Doktycz et al., 1992). In particular, single-stranded hairpin molecules are favorable for these thermodynamic studies because they form stable partially paired duplexes that tend to melt in monomolecular transitions. The structure and overall physical properties of synthetic DNA fragments forming single-stranded hairpin molecules have been reported earlier (Marky et al., 1983a; Summers et al., 1985; Wemmer et al., 1985; Haasnoot et al., 1986; Hare & Reid, 1986; Ikuta et al., 1986; Gupta et al., 1987; Chattopadayaya et al., 1988; Garcia et al., 1988; Wolk et al., 1988; Williamson & Boxer, 1989 a,b; Garcia et al., 1990; Paner et al., 1990; Rentzeperis et al., 1991), as have the effects of sequence and loop size on hairpin stability (Amaratunga et al., 1989; Benight et al., 1989; Erie et al., 1987; Hilbers et al., 1985; Senior et al., 1988; Wemmer & Benight, 1985; Xodo et al., 1986, 1988 a,b; Amaratunga et al., 1992; Antao & Tinoco, 1992). More recently, Benight's group have used a set of ligated dumbbells to calculate the relative contributions of each DNA base pair stacking interaction, which can be used to predict the overall stability of a DNA molecule from its sequence (Doktycz et al., 1992).

In designing new drugs that recognize specific DNA sequences, it is important to have thermodynamic information on the DNA–ligand interactions as well as information on the structure of the complexes. Netropsin belongs to the class of minor groove ligands that show strong sequence specificity (Luck et al., 1974; Wartell et al., 1974; Zimmer, 1975). The

† Supported by Grant GM-42223 from the National Institutes of Health. Preliminary results of this work have been submitted (by J.H.) to the 50th Science Talent Search, Sponsored by the Westinghouse Electric Corporation and Science Service, 1991.

* To whom correspondence should be addressed.

0006-2960/93/0432-2564$04.00/0

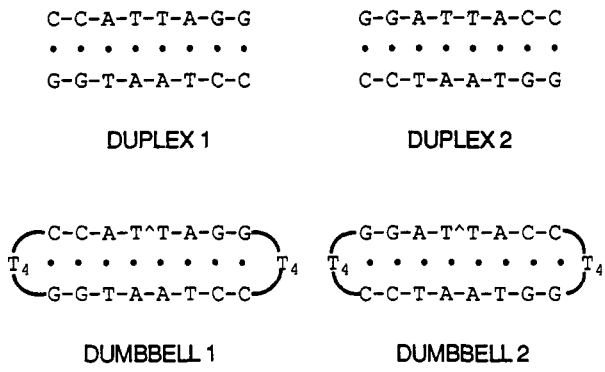

FIGURE 1: Sequences of deoxyoligonucleotides.

molecular basis for the formation of netropsin–DNA complexes has been under intensive investigation by a variety of techniques (Patel & Canuel, 1977; Berman et al., 1979; Patel, 1979, 1982; Marky et al., 1983b, 1985; Kopka et al., 1985; Dervan, 1986; Marky, 1986; Zimmer & Wanhert, 1986; Marky & Breslauer, 1987; Bresslauer et al., 1988; Ward et al., 1988; Coll et al., 1989; Marky & Kupke, 1989). This ligand binds in the minor groove of double-helical B-DNA. The strong specificity for A·T base pairs is attributed to both the specific formation of hydrogen bonds between the amide protons of netropsin with the atomic groups N3 of adenine and O2 of thymine of the nucleotide edges facing the floor of this groove (Kopka et al., 1985; Coll et al., 1989) and van der Waals contacts between the methyl and pyrrole groups of netropsin and the sugar–phosphate backbone of DNA resulting from its tight fit in the minor groove. However, the specific contributions of sequence and conformational effects to the overall stability of the complex have yet to be completed.

Previously, we have reported that the overall physical properties of an unligated dumbbell molecule corresponded to the sum of its component single hairpins with the exeption of an increase in cooperativity that resulted from the ionic coupling of the two hairpin domains (Rentzeperis et al., 1991). In an attempt to evaluate the relative contribution of loops and nicks to the melting behavior of an unligated DNA dumbbell and their response to ligand binding, we report here on the thermodynamics of the helix–coil transition of two dumbbell molecules and their corresponding core duplexes (Figure 1) as well as on the interaction of these molecules with the minor groove ligand netropsin.

EXPERIMENTAL PROCEDURES

Materials

All four oligonucleotides (Figure 1) were synthesized on an ABI 380-B automated synthesizer, using standard phosphoramidite chemistry (Caruthers et al., 1982), purified by HPLC, and desalted on a Sephadex G-10 exclusion chromatography column. Extinction coefficient of the oligomers in single strands were calculated at 25 °C using the tabulated values of the dimers and monomer bases (Cantor et. al., 1979) and estimated at high temperatures by extrapolation of the absorbance vs temperature curves of the single strands to 25 °C. The concentrations of the oligomers were determined in water using the following extinction coefficients in single strands at 260 nm and 95 °C (in $mM^{-1}\cdot cm^{-1}$): 78.9 for d(GGATTACC); 79.5 for d(GGTAATCC); 79.4 for d(CCATTAGG); 77.6 for d(CCTAATGG); 216 for d(TACCT$_4$GGTAATCCT$_4$GGAT); and 226 for d(TAGGT$_4$CCTAATGGT$_4$CCAT). Netropsin hydrochloride from Serva Biochemicals was used without further purification; its concentration was determined in water using $\epsilon_{296,25°C} = 21\,500$ $M^{-1}\cdot cm^{-1}$. All other chemicals were reagent grade. The buffer solutions consisted of 10 mM NaP_i, pH 7.0, 0.1 mM Na_2-EDTA, adjusted to the desired ionic strength with NaCl. Stock solutions of the oligomers were prepared by dissolving directly dry and desalted oligomers in the appropriate buffer.

Methods

Temperature-Dependent UV Spectroscopy. Absorbance versus temperature profiles (melting curves) in appropriate solution conditions were measured at 260 nm with a thermoelectrically controlled Perkin-Elmer 552 spectrophotometer, interfaced to a PC-XT computer for acquisition and analysis of experimental data. The temperature was scanned at a heating rate of 1.0 °C/min. From these melting curves, the transition temperature, T_m, and van't Hoff enthalpy, ΔH_{vH} were obtained using standard procedures reported elsewhere (Marky & Breslauer, 1987; Rentzeperis et al., 1991: Zieba et al., 1991). These melting curves were carried out as a function of total strand concentration and for salt dependence studies at a constant strand concentration of 6 μM in buffer with an overall NaCl concentration of 0–100 mM. The slopes of the plots of T_m vs log [Na^+] are proportional to the thermodynamic release of counterions, Δn_{Na^+}. The relevant equation is (Record et al., 1978)

$$dt_m/d \ln [Na^+] = 0.9(RT_m^2/\Delta H°_{cal})\Delta n_{Na^+} \quad (1)$$

where the value of 0.9 is a factor of converting mean ionic activities to concentrations; the term in parentheses is measured directly in differential scanning calorimetric experiments; and R is the gas constant equal to 1.987 cal·K^{-1}·mol^{-1}. The Δn_{Na^+} values are normalized per phosphate by taking into account the appropriate number of phosphates in the helical state of these molecules, i.e., neglecting the loop phosphates.

Calorimetry. Excess heat capacity as a function of temperature (DSC melts) for each oligomer was measured with a Microcal MC-2 differential scanning calorimeter (Northampton, MA). This technique allows us to obtain standard thermodynamic profiles ($\Delta H°$, $\Delta S°$, $\Delta G°$) and model-dependent enthalpies, $\Delta H°_{vH}$, of the helix–coil transition of oligonucleotides as described earlier (Marky & Breslauer, 1987).

The heats for the interaction of netropsin with each oligomer duplex were measured directly by titration calorimetry using the Omega calorimeter from Microcal Inc. Netropsin solutions were used to titrate the oligonucleotide duplex with a 100-μL syringe. Complete mixing was effected by stirring of the syringe paddle at 400 rpm. The concentration of ligand in the syringe was generally 25 or 50 times higher than any of the oligomer solutions in the reaction cell. The reference cell of the calorimeter was filled with water, and the instrument was calibrated by means of a known standard electrical pulse. Typically, 12–28 injections of 5 or 6 μL each were performed in a single titration. The area under the resulting peak following each injection is proportional to the heat of interaction, Q. When corrected for the titrant dilution heat and normalized by the concentration of added titrant, Q is equal to the binding enthalpy, $\Delta H°_b$. The precision on the heat of each injection is less than 0.5 μcal. Analysis of the calorimetric binding isotherm, as described in a latter section, allows us to obtain, in addition to the binding enthalpy, binding affinities and the overall stoichiometry of the complexes.

Circular Dichroism (CD). The CD spectrum of each netropsin–DNA complex at several [netropsin]/[duplex] ratios was obtained on an Aviv-60DS spectropolarimeter equipped

with a Hewlett Packard thermoelectrically controlled cell holder. These spectra allowed us to define qualitatively the global conformational state asssumed by each oligomer duplex and to verify the formation of single bound species by the presence of isoelliptic points in the overlay of the spectra as a function of the ligand/DNA molar ratios. The stoichiometry of the netropsin–DNA complexes was obtained by following the induced Cotton effect of the bound ligand at 310 nm as a function of the netropsin/DNA molar ratio.

Determination of Ligand Association Constants. Netropsin association constants, K_b, were measured using two different methods: (1) from the increase in thermal stability of the saturated ligand–DNA complexes relative to the free oligomer duplexes, and (2) from analysis of the calorimetric binding isotherms.

In the first method, the thermal stabilization of the netropsin–DNA complex, ΔT_m, relative to free duplex follows the equation (Crothers, 1971)

$$\Delta T_m = (T^\circ_m T_m N R/\Delta H^\circ_{cal}) \ln (1 + K a_L) \qquad (2)$$

where T°_m and T_m are the transition temperatures of the free and fully saturated duplexes, respectively; ΔH°_{cal}, the dissociation enthalpy of 5 base pairs (4 base-pair stacks) that constitute one binding site, is estimated from the nearest-neighbor enthalpies (Breslauer et al., 1986); a_L, the activity of the free ligand, is assumed equal to half of the total concentration of netropsin at T_m; N, the apparent number of binding sites per oligomer duplex, is equal to one in all cases. Ligand binding affinities are extrapolated to 5 °C by the van't Hoff equation:

$$d \ln K_b/d(1/T) = -\Delta H^\circ_b/R \qquad (3)$$

where ΔH°_b is assumed to be independent of temperature (Marky et al., 1985).

The second method is based on the binding of a ligand to oligomers containing one binding site (for the core duplexes) or two independent binding sites, the central A·T base pairs of the stem and the thymine loops (for the dumbbells), respectively. Each type of site is characterized by an equilibrium constant, K_b, binding enthalpy, ΔH°_b, and apparent number of ligands per binding site, n. The calorimetric binding isotherm is just the dependence of the total heat, Q_T, on the total concentration of ligand added, X_{Tot}. The above three parameters for each type of site are determined from the resulting calorimetric binding isotherm iteractively using the Marquardt algorithms as has been described previously (Wiseman et al., 1989). To facilitate the fitting procedures, two data files with different oligomer concentration were analyzed simultaneously. The initial fitting procedure, which is part of the software of the calorimeter provided by Microcal Inc., is to let all three parameters float or to fix either the enthalpy or n parameters or both until the lowest standard deviation of the fit is obtained; all approaches resulted in similar overall parameters. Comparison of the K_b values obtained from both methods are in excellent agreement.

RESULTS

Helix–Coil Transition of Deoxyoligonucleotides

UV-Melting Curves. The helix–coil transition of the ordered structures formed by the two dumbbells and the corresponding core duplexes were characterized initially by UV-melting curves. The transition temperatures and the corresponding van't Hoff enthalpies for all four oligomers are listed in Table I. The melting of all four molecules occurs in monophasic transitions (see Figure 2a,b). The dumbbells melt with T_m's 19 °C and 31 °C higher than the T_m's of the corresponding duplexes in each set. All four molecules show broad transitions with van't Hoff transition enthalpies of 51 kcal·mol^{-1} for the duplexes and 31 kcal·mol^{-1} for the dumbbells. In these optical melts, a 10-fold increase in oligomer concentration has no effect on the T_m of the dumbbell molecules. This is consistent with the unimolecular melting of single-stranded hairpins (see Figure 2c). On the other hand, the T_m of each duplex increases with increasing strand concentration, a result characteristic of the melting of bimolecular complexes.

Calorimetry and Nature of the Transitions. Typical excess heat capacity versus temperature profiles are presented in Figure 3. The T_m, ΔH°_{cal} and ΔH°_{vH} values obtained from

Table I: Spectroscopic and Calorimetric Melting Results[a]

	UV		calorimetry		
oligomer	T_m (°C)	ΔH°_{vH} (kcal·mol^{-1})	T_m (°C)	ΔH°_{vH} (kcal·mol^{-1})	ΔH°_{cal} (kcal·mol^{-1})
duplex 1	16.5	52 (50)	30.7	54	54.2
dumbbell 1	35.4	29	36.2	32	63.1
duplex 2	13.9	54 (52)	27.9	53	54.9
dumbbell 2	44.7	33	45.0	36	61.2

[a] In 10 mM NaP_i buffer, 0.1 mM Na_2EDTA at pH 7.0. All T_m's are within ±0.5 °C; ΔH°_{vH} are within ±7% of absolute values; and ΔH°_{cal} are within ±3% of absolute values. The T_m values correspond to strand concentrations of 10 μM for the optical melts and 210 μM (in duplex) and 220 μM (dumbbells) for the DSC melts. The ΔH°_{vH} values in parentheses were obtained from plots of the concentration dependence of the T_m.

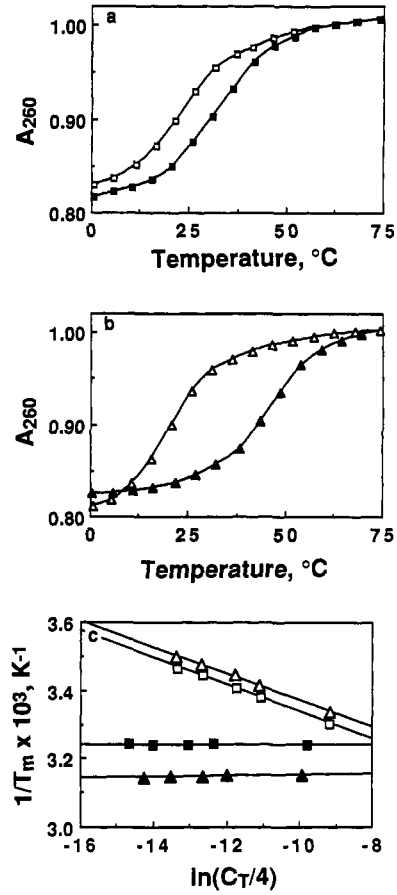

FIGURE 2: (a, b) Normalized melting curves of duplexes (60 μM in strand concentration) and dumbbells (30 μM in strand concentration) in 10 mM NaP_i buffer, 0.1 mM Na_2EDTA, at pH 7. (c) Dependence of T_m on strand concentration. Symbols: duplex 1 (□), dumbbell 1 (■), duplex 2 (△), and dumbbell 2(▲).

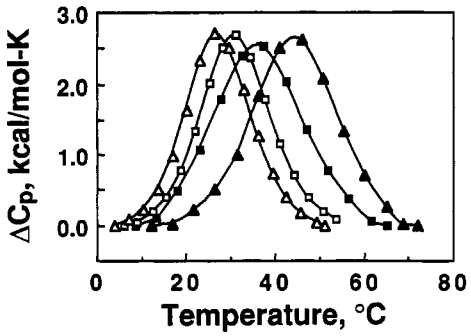

FIGURE 3: Typical excess molar heat capacity curves relative to buffer consisting of 10 mM NaP_i buffer, 0.1 mM Na_2EDTA at pH 7. Symbols: duplex 1 (□), dumbbell 1 (■), duplex 2 (△), and dumbbell 2 (▲). At strand concentrations of 420 μM and 220 μM for the duplexes and dumbbells, respectively.

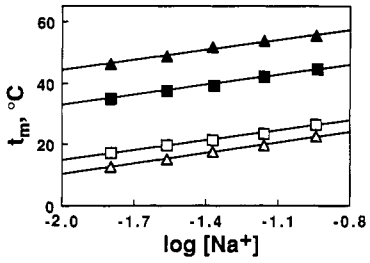

FIGURE 4: Dependence of T_m on salt concentration for oligonucleotides in 10 mM NaP_i buffer, 0.1 mM Na_2EDTA at pH 7 adjusted to the desired NaCl concentration. Symbols: duplex 1 (□), dumbbell 1 (■), duplex 2 (△), and dumbbell 2 (▲).

these curves are listed in Table I. Figure 3 shows DSC melts that are all monophasic with no changes in heat capacities within initial and final states. For the dumbbells, in spite of the 70-fold increase in strand concentration relative to the concentration used in optical melts, the T_m remains the same. The average $\Delta H°_{cal}$ of 54.2 kcal·mol^{-1} for duplex 1 and 54.9 kcal·mol^{-1} for duplex 2, determined in 0.1 M NaCl, are in good agreement with the enthalpies of 59 and 58 kcal·mol^{-1} estimated from nearest-neighbor parameters in 1 M NaCl (Breslauer et al., 1986), respectively. The dumbbells have $\Delta H°_{cal}$ values that are 8.9 and 6.3 kcal·mol^{-1} higher than the corresponding duplex of each set. These enthalpic differences can be explained in terms of base-stacking contributions of the loop thymines at both ends of the duplexes and the presence of a small percentage of frayed G·C ends in the duplexes. Comparison of the model-dependent $\Delta H°_{vH}$'s calculated from calorimetric or optical experiments and $\Delta H°_{cal}$ values for a given molecule allows us to draw conclusions about the nature of the transitions (Marky & Breslauer, 1987). In low salt buffer solution, we obtained $\Delta H°_{vH}/\Delta H°_{cal}$ ratios of 1 and 0.97 for the duplexes and 0.51 and 0.59 for each dumbbell, respectively; the $\Delta H°_{vH}$ values correspond to the melting of one cooperative unit size. Therefore, the duplexes melt in two-state transitions and the dumbbells melt in apparent non-two-state transitions. In the monophasic transitions of the dumbbells, this corresponds roughly to the melting of half of each molecule. Their unusual $\Delta H°_{vH}/\Delta H°_{cal}$ values suggest the coupled melting of both halves of these molecules.

Salt Dependence of T_m and Overall Counterion Release. Figure 4 shows plots of T_m versus log [Na^+]. We obtained values ranging from 10.9 to 12.5 for the slopes of such plots (see Table II). This weak dependence on salt concentration is characteristic of ion release that occurs in oligomeric duplexes (Erie et al., 1987; Rentzeperis et al., 1991; Zieba et al., 1991). For the calculation of Δn_{Na^+} per phosphate, we have taken into account just the helical phosphates: 13 phosphate groups for the dumbbells and 14 for the duplexes. The resulting Δn_{Na^+} values are included in Table II. The higher Δn_{Na^+} values of the dumbbells suggest that the loop phosphates behave electrostatically as partially helical. Most likely, the phosphate groups located at the ends of the core duplexes are participating in the melting of these molecules; i.e., the dumbbells melt electrostatically as decamers as has been reported previously for oligomers of this length (Zieba et al., 1991).

Table II: Thermodynamic Profiles for the Formation of Duplexes[a]

oligomer	$\Delta G°$ (kcal/mol)	$\Delta H°$ (kcal/mol)	$T\Delta S°$ (kcal/mol)	$dt_m/d \log [Na^+]$ (K)	Δn_{Na^+} (mol of Na^+/P_i)
duplex 1	−4.6	−54.2	−49.6	10.9	0.11
dumbbell 1	−6.4	−63.1	−56.7	11.0	0.14
duplex 2	−4.2	−54.9	−50.7	11.8	0.12
dumbbell 2	−7.7	−61.2	−53.5	12.5	0.14

[a] In 10 mM sodium phosphate buffer, 0.1 mM EDTA at pH 7.0 and 5 °C. $\Delta G°$ values are within 5%, $\Delta H°$ are within 3%, and $T\Delta S°$ are within 8%. The slopes of the t_m vs log [Na^+] plots were obtained by least-squares analysis with at least 99% confidence level. The values of Δn_{Na^+} are ±5.0%.

Thermodynamic Profiles at 5 °C. For suitable comparisons, Table II lists standard thermodynamic profiles ($\Delta G°$, $\Delta H°$, and $T\Delta S°$) for the formation of each molecule at 5 °C, a temperature at which all molecules are fully ordered. The $\Delta S°$ and $\Delta G°$ are calculated directly from DSC experiments with the following equations: $\Delta S° = \int (\Delta C_p/T)\, dT$ and $\Delta G° = \Delta H°_{cal} - 278.15\ \Delta S°$; in the Gibbs equation, both the enthalpy and entropy are assumed independent of temperature, i.e., $\Delta C_p = 0$. For all four molecules, the $\Delta G°$ values determined in this way follows the equation: $\Delta G° = \Delta H°_{cal}(1 - 278.15/T_m)$ closely, which is rigorously true for the monomolecular unfolding of the dumbbells. As expected, both duplexes exhibit similar thermodynamic profiles (see Table II). At concentrations used in the DSC experiments, we obtained favorable $\Delta G°$ terms ranging from −4.2 to −7.7 kcal·mol^{-1} that resulted from a partial compensation of favorable enthalpies with unfavorable entropies. In the two sets of molecules, the stabilization of the dumbbells by −1.8 and −3.5 kcal·mol^{-1}, relative to the corresponding duplexes, is enthalpic in origin and is accompanied by slightly higher differential counterion uptake.

Binding of Netropsin to Deoxyoligonucleotides

Stoichiometry of Complexes. The addition of netropsin to an oligomer duplex solution results in changes of the overall CD spectrum. In particular, we note the presence of an extra band at ~310 nm that corresponds to the induced Cotton effect of the bound ligand (see Figure 5a). We have used this wavelength to follow the binding of netropsin to each oligomer. The resulting titrations are shown in Figure 5b,c. From this optical observable, we obtained 1:1 complex stoichiometries of the ligand with all four oligomers, as seen in the breaks of these curves, and which correspond to the strong binding of netropsin to the central core of A·T base pairs of the duplexes and dumbbells. However, as will be discussed in the calorimetry section, the terminal GC base pairs and the adjacent loop at each end of the dumbbell molecules can accommodate more ligands. These additional weaker binding sites can be seen by comparing the slopes of the lines of the upper portions of the CD titrations. The octameric duplexes show lines with negative slopes while the dumbbells show flat upper lines. This small change is in agreement with the much lower magnitude of both the induced Cotton effect and K_b

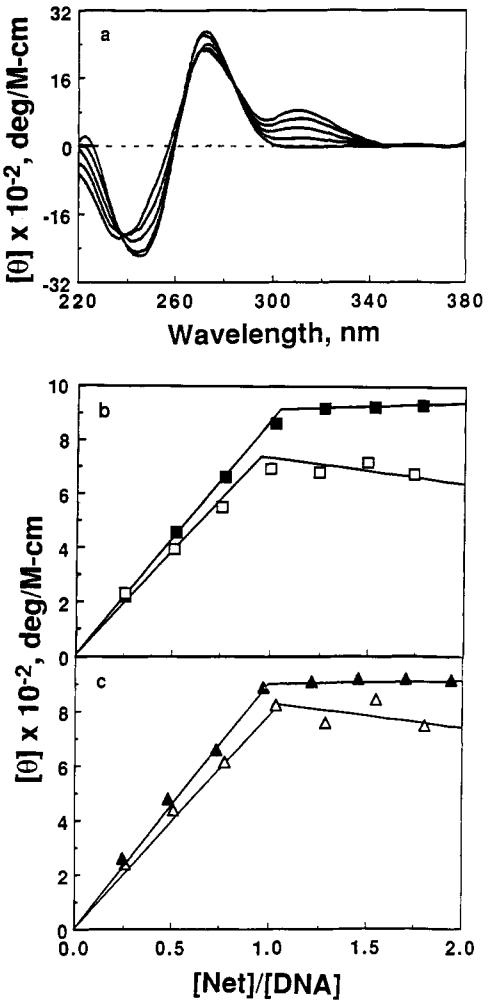

FIGURE 5: (a) Typical spectra of netropsin–dumbbell 1 complexes at several increasing concentration of netropsin. (b, c) Circular dichroism titrations curves in 10 mM NaP_i buffer, 0.1 mM Na_2-EDTA, 0.1 M NaCl at pH 7. Symbols: duplex 1 (□), dumbbell 1 (■), duplex 2 (△), and dumbbell 2 (▲). Conditions: 2.7 mL of oligomer solution in 1-cm quartz cell at strand concentration of 15 μM (duplexes) and 7.5 μM (dumbbells) titrated with 10-μL aliquots of 0.5 mM solution of netropsin.

values for netropsin binding to G·C base pairs (Luck et al., 1974).

Netropsin Binding Affinities. Table III lists the specific parameters used to calculate K_b from UV-melting curves and the resulting binding affinities at two different salt concentrations. In low salt, we obtained similar K_b values of $\sim 10^8$ for all four molecules, which are consistent with the high specificity of netropsin for the central core of four A·T base pairs. With a 10-fold increase in the NaCl concentration, these K_b's decreased to $\sim 10^7$. The similarity of these binding affinities for all four molecules strongly indicates that the sequences of the binding sites that are contained in the duplexes (GATTAC/GTAATC and CATTAG/ CTAATG), and in the unligated dumbbells with nicks (GAT^TAC/GTAATC and CAT^TAG/CTAATG) constitute identical binding sites. Thus, netropsin recognizes the A·T base pairs at the nick point as normal helical base pairs, that is with similar base-stacking interactions and local helical parameters. One difference in the binding of netropsin to these two types of helical conformations is their response to salt concentration. The values of the slopes of ln K_b vs ln [Na^+] are similar and equal to 1.1 for the duplexes and 1.0 for the dumbbells (see Figure 6a,b); these values are consistent with the lower charge

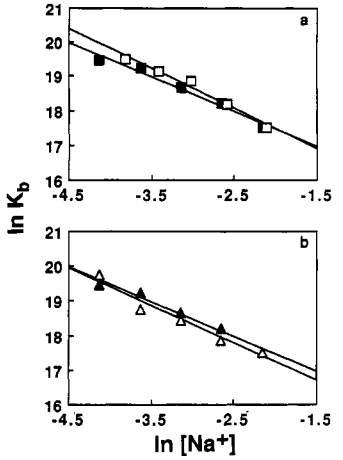

FIGURE 6: Salt dependence of netropsin binding affinities with oligomers in 10 mM NaP_i buffer, 0.1 mM Na_2EDTA at pH 7 and 5 °C, and adjusted to the desired NaCl concentration. Panel a: duplex 1 (□) and dumbbell 1 (■). Panel b: duplex 2 (△) and dumbbell 2 (▲).

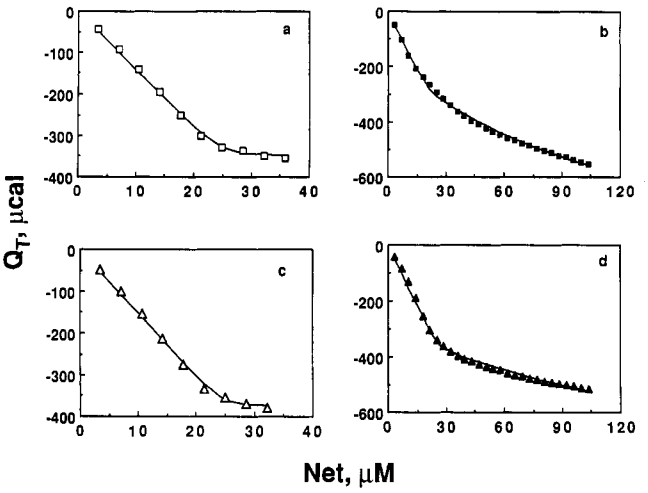

FIGURE 7: Fitted calorimetric binding isotherms curves in 10 mM NaP_i buffer, 0.1 mM Na_2EDTA, 0.1 M NaCl at pH 7 and 5 °C. Conditions: duplex 1 (a), dumbbell 1 (b), duplex 2 (c) and dumbbell 2 (d); 1.4 mL of oligomer solution at strand concentration of 40 μM (duplexes) and 20 μM (dumbbells) titrated with 5-μL aliquots of a 1 mM solution of netropsin.

density of all four duplexes. The small difference of 0.1 may be explained in terms of the absence of a phosphate group at the nick point of the dumbbells.

Titration Calorimetry. The resulting integral heat as a function of total added ligand for all netropsin–oligomer systems is shown in Figure 7. Molar binding enthalpies for the high affinity sites were calculated by averaging the heats of the first few points of these isotherms (or from the fits of these calorimetric titrations) which correspond to complete binding of ligand. These values, obtained at two different salt concentrations, are listed under the ΔH_b columns in Table IV. Inspection of this column shows that binding of netropsin to all four molecules is accompanied with an exothermic enthalpy of −10.3 kcal·mol^{-1} to −10.9 kcal·mol^{-1} that is independent of salt concentration, sequence, and oligomer conformation. Furthermore, the analysis of the calorimetric binding isotherms at the high salt concentration resulted in binding affinities that were in good agreement with the ones obtained from optical melts; at the lower salt concentration, we were unable to fit all four molecules because the K_b values of $\sim 10^8$ are above the limit of analysis of this method. In addition, in these calorimetric titrations we were able to

Table III: Binding Affinities for Netropsin Binding to Oligomer Duplexes[a]

oligomer	T°_m (K)	T_M (K)	N (bp)	ΔH°_{cal} (kcal·mol^{-1})	ΔH°_b (kcal·mol^{-1})	K_b (M^{-1})
duplex 1	290.2	311.6	1	−31.5	−10.6	2.6 (±1.4) × 10^8
	(299.5)	(310.5)	(1)	(−31.5)	(−10.8)	(2.6 (±1.1) × 10^7)
dumbbell 1	308.7	324.1	1	−31.5	−10.6	2.8 (±1.3) × 10^8
	(319.3)	(326.5)	(1)	(−31.5)	(−10.4)	(4.2 (±2.2) × 10^7)
duplex 2	287.0	316.7	1	−30.2	−10.8	3.6 (±2.0) × 10^8
	(301.0)	(318.5)	(1)	(−30.2)	(−10.9)	(4.2 (±2.0) × 10^7)
dumbbell 2	317.4	335.5	1	−30.2	−10.4	2.9 (±1.4) × 10^8
	(327.4)	(335.2)	(1)	(−30.2)	(−10.3)	(4.2 (±2.2) × 10^7)

[a] Values were taken in 10 mM sodium phosphate buffer, 0.1 mM Na_2EDTA, at pH = 7.0 and 5 °C (values in parentheses are with additional 0.1 M NaCl). Transition temperatures are within ±0.5 °C and 10% for N.

Table IV: Fitting Analysis of Calorimetric Binding Isotherms

	strong site			weak site			
oligomer	n (mol of ligand/ mol of DNA)	ΔH°_b (kcal·mol^{-1})	K_b (M^{-1})	n (mol of ligand/ mol of DNA)	ΔH°_b (kcal·mol^{-1})	K_b (M^{-1})	σ (%)
duplex 1		−10.6					
	(1.08)	(−10.8)	(1.1 × 10^7)				(4.2)
dumbbell 1	1.1	−10.6	>1.0 × 10^8	3.8	−4.7	3.6 × 10^5	6.9
	(0.9)	(−10.4)	(1.7 × 10^7)	(3.9)	(−3.4)	(5.8 × 10^4)	(7.2)
duplex 2		−10.8					
	(1.0)	(−10.9)	(1.3 × 10^7)				(6.3)
dumbbell 2	1.1	−10.4	>1.0 × 10^8	3.8	−5.5	1.1 × 10^5	8.0
	(1.1)	(−10.3)	(2.2 × 10^7)	(3.9)	(−3.4)	(1.3 × 10^4)	(8.0)

[a] Values taken in 10 mM sodium phosphate buffer, 0.1 mM Na_2EDTA, at pH = 7.0 and 5 °C. Values in parentheses are with the inclusion of 0.1 M NaCl. σ is the standard deviation of the nonlinear fits.

Table V: Thermodynamic Profiles for Netropsin Binding to Oligomers[a]

oligomer	site	ΔG°_b (kcal·mol^{-1})	ΔH°_b (kcal·mol^{-1})	$T\Delta S^\circ_b$ (kcal·mol^{-1})	d ln K_b/d ln [Na$^+$]
duplex 1	strong	−10.7	−10.6	+0.1	−1.1
		(−9.4)	(−10.8)	(−1.4)	
dumbbell 1	strong	−10.7	−10.6	+0.1	−1.0
		(−9.7)	(−10.4)	(−0.7)	
	weak	−7.1	−4.7	+2.4	−0.9[b]
		(−6.1)	(−3.4)	(+2.7)	
duplex 2	strong	−10.9	−10.8	+0.1	−1.1
		(−9.7)	(−10.9)	(−1.2)	
dumbbell 2	strong	−10.8	−10.4	+0.4	−1.0
		(−9.7)	(−10.3)	(−0.6)	
	weak	−6.4	−5.5	+0.9	−1.1[b]
		(−5.2)	(−3.4)	(+1.8)	

[a] Values were taken in 10 mM sodium phosphate buffer, 0.1 mM Na_2EDTA at pH = 7.0 and 5 °C. Values in parentheses were with inclusion of 0.1 M NaCl. The ΔG°_b values are within 5%, ΔH°_b are within ±3%, $T\Delta S^\circ_b$ are within ±8%, and d ln K_b/d ln [Na$^+$] are within ±6%. [b] These values were obtained from calorimetric titration experiments at two salt concentrations.

detect secondary weaker sites for netropsin in the dumbbells (see Table IV). These sites are located at each end of the dumbbells and are composed either of two G·C pairs in the stem and the adjacent thymine loops or of just the constrained thymines of the loops. The interesting observation is that each of these sites is able to accommodate two ligand molecules. In low salt buffer, these sites are characterized with K_b's of $\sim 10^5$ and exothermic ΔH_b's of −4.7 kcal·mol^{-1} to −5.5 kcal·mol^{-1}, and increase in salt concentration reduces the K_b's to $\sim 10^4$ and ΔH_b's to −3.4 kcal·mol^{-1}.

Thermodynamic Profiles for Netropsin Binding. Values for the thermodynamic profiles for the binding sites of netropsin to each of the four oligomer duplexes at 5 °C in two different salt concentrations are listed in Table V. In this table, we have tabulated standard thermodynamic profiles, ΔG°_b, ΔH_b, $T\Delta S^\circ_b$, and d ln K_b/ d ln [Na$^+$]. The ΔG°_b were derived from the values of K_b according to $\Delta G^\circ_b = -RT \ln K_b$. The entropy changes, $T\Delta S^\circ_b$, were then calculated from the Gibbs equation. For the strong binding sites located at the center of the molecules, we obtained ΔG°_b of −10.8 kcal·mol^{-1}. These values decreased to −9.6 kcal·mol^{-1} with a 10-fold increase in NaCl concentration. In all cases these ΔG°_b terms correspond to binding processes that are primarily enthalpically driven. However, the decrease in the ΔG°_b is entropically driven when there is an increase in salt concentration and thus corresponds to a less favorable entropy term, $\Delta(T\Delta S^\circ_b)$ of −1.5 kcal·mol^{-1}, consistent with processes driven by electrostatic effects (Manning, 1978; Record et al., 1978). For the secondary sites of the dumbbells, we obtained an average ΔG°_b of −6.8 kcal·mol^{-1} decreasing to −5.7 kcal·mol^{-1} with a 10-fold increase in the NaCl concentration and ΔH°_b's values of −5.1 kcal·mol^{-1} and −3.4 kcal·mol^{-1} for the low and high salt conditions, respectively. This decrease in ΔG°_b with an increase in salt concentration is enthalpically driven, $\Delta\Delta H^\circ_b = 1.7$ kcal·mol^{-1}, and is due to the increase in hydrophobic interactions between two netropsin molecules in the same binding site.

DISCUSSION

Formation of Intramolecular Dumbbells and Intermolecular Duplexes. The sequences of the dumbbells were

designed in such a way to favor the exclusive formation of intramolecular duplexes. The formation of intermolecular duplexes would involve four G·C base pairs interspaced by three internal loops of 8 bases each, which would render them unstable. The T_m's for the helix–coil transition of dumbbells remain constant despite the 50–100-fold increase in strand concentration: 5 μM to 150 μM (UV and DSC melts). This confirms the formation of unimolecular complexes at low temperatures. On the other hand, the non-self-complementary duplexes show characteristic bimolecular shifts to higher temperatures with increasing strand concentration. Furthermore, the higher T_m's of the dumbbells relative to duplexes, together with the similarity of the transition enthalpies and counterion release of all molecules, provide strong evidence of the exclusive formation of intramolecular dumbbells.

Thermodynamic Contribution of the Thymine Loops. The presence of the thymine loops in the dumbbells increases the thermal stability of these molecules. This increase in thermal stability, relative to the core duplex, depends on the concentration of the octameric duplexes (see Figure 2c) and on the sequence of the duplex–loop interface (5′-G-T-3′ and 5′-C-T-3′). Therefore, we explain this differential stability in terms of two contributions: an entropic contribution due to differences in the nucleation parameters (monomolecular vs bimolecular) and an enthalpic contribution due to formation of additional base-stacking interactions between the thymines in the loop and/or the thymines with the G·C base pairs at the ends of the duplexes. For instance, at the concentrations used in the calorimetric experiments, the stabilization of each dumbell relative to its counterpart duplex corresponds to $\Delta\Delta G^\circ = -1.8$ kcal·mol^{-1}, $\Delta\Delta H^\circ = -8.9$ kcal·mol^{-1}, and $\Delta(T\Delta S^\circ) = -7.1$ kcal·mol^{-1} for dumbbell 1; and $\Delta\Delta G^\circ = -3.5$ kcal·mol^{-1}, $\Delta\Delta H^\circ = -6.3$ kcal·mol^{-1}, and $\Delta(T\Delta S^\circ) = -2.8$ kcal·mol^{-1} for dumbbell 2. The higher stability of the dumbbells at DSC concentrations, 5.5 °C–17.1 °C, is primarily enthalpically driven and corresponds in this case to increased stacking interactions of the constrained thymines in the loops and/or between the loop thymines and the G·C base pairs at both ends of the stem (Hare & Reid, 1986; Hilbers et al., 1991; Gupta et al., 1987). These enthalpy contributions correspond to –4.5 kcal·mol^{-1} per loop for the 5′-G-T4-C-3′ loop and –3.1 kcal·mol^{-1} per loop for the 5′-C-T4-G-3′ loop. At optical concentrations of 10 μM (in strands) the differential stability of the dumbbells increases to 18.9 °C and 30.8 °C in each set. The additional stability of ~13.6 °C reflects the more favorable entropic contribution of nucleating an intramolecular dumbbell relative to the bimolecular nucleation of a duplex and corresponds to a $\Delta\Delta G^\circ$ of approximately –2.6 kcal.

Thermodynamic Contribution of Nicks. We obtained similar thermodynamic profiles for the binding of netropsin to the central core of four A·T base pairs of the duplexes with nicks and without nicks. This ligand is recognizing both sequences in an equal way with a smaller electrostatic component for the dumbbells. This can be seen from their lower decreases in K_b with increased salt concentration. This suggests that the stacking interactions and base-pair alignment of the T^T/AA base-pair stack (with the nick at the center) is very similar to the TT/AA base-pair stack of a regular helical segment. Therefore, the presence of the loops does not influence the local helical structure at the center of the dumbbells, in agreement with previous NMR investigations of a dumbbell containing a C^G/GC nick (Snowden-Ifft & Wemmer, 1990). Our finding is in disagreement with previous results of a dumbbell with a stem sequence of GGAA^TTCC which could not be successfully ligated presumably due to the misalignment of the bases at the nick point (Erie et al., 1987). However, Ashley and Kushlan were able to synthesize a closed molecule with identical sequence that folded into a dumbbell (Ashley & Kushlan, 1991). What is surprising in the melting of the dumbbells reported in this paper is the low values of ΔH_{vH} (optical and calorimetric). These values correspond to the melting of only half of each molecule. Thus, the dumbbells respond to an increase in temperature by the cooperative unfolding of the two halves of each molecule. The presence of the nick is exactly at the center of each dumbbell allows this cooperative behavior; each half contains exactly the same sequence, and the shapes of their melting profiles are symmetric. This effect is different to one reported earlier in which the whole molecule melted in a two-state transition (Erie et al., 1987, 1989); the contrast in behavior may be due to sequence differences; i.e., the AA/TT base-pair stack is more stable than the AT/TA base-pair stack. Furthermore, the thermal stability of the dumbbells corresponds roughly to that of hairpins containing four base pairs in the stem (Rentzeperis et al., 1991; Antao et al., 1991) and allows us to postulate that the presence of a nick in a double-helical molecule will disrupt the cooperative communication between DNA helical segments at opposite sides of the nick with the overall lowering of the thermal stability of the molecule.

The Inclusion of Loops Creates Additional Netropsin Binding Sites. The presence of the loops provides additional weaker sites for netropsin in both dumbbells as detected in the fitting of the calorimetric binding curves. Their thermodynamic parameters are similar to those of netropsin binding to GC sequences (Marky & Breslauer, 1987) and probably correspond to the nonspecific binding of netropsin. Our thermodynamic studies cannot predict the actual structure of these weaker sites. These sites could contain the two G·C base pairs at each end of the duplex plus the adjacent two thymines of the loops forming a local duplex structure of nearly three base pairs. Alternatively, the constrained thymines of the loops could form these sites as reported earlier with ethidium and propidium (Marky, 1990). However, we obtained an average value of –1.0 mol of Na^+/mol of ligand for the slopes of ln K_b vs ln [Na^+] plots for these sites, indicating that they have double-helical structure. In addition, these secondary sites are able to accommodate two netropsin molecules, in a way similar to the side-by-side binding of distamycin A to A·T base pairs reported previously (Pelton & Wemmer, 1989, 1990). The structures of these complexes are currently under study using NMR techniques.

CONCLUSIONS

We have thermodynamically characterized the helix–coil transition of two dumbbells and the corresponding core duplexes and their interaction with the minor groove ligand netropsin. Our standard thermodynamic parameters of formation for these molecules indicate that the overall increase in the stability of the dumbbells relative to the core duplexes is the result of differences in their nucleation entropies and favorable stacking interactions of the loop thymines, as seen by the increase of both the exothermicity of the enthalpy and overall charge density. However, the transition free energy values of the dumbbells correspond to those of single hairpins containing only four base pairs in the stem. An effect due to the inclusion of a nick in the center of the dumbbells, which is not affecting the overall stacking of the T^T/AA base pair at the center, is that it interrupts the cooperative melting of the whole molecule. The increased response of the dumbbells (relative to duplexes) to salt and the additional association of

netropsin molecules to the ends of the dumbbells strongly suggest that the loop thymines are constrained, forming additional stacked base pairs in a double-helical geometry.

ACKNOWLEDGMENT

We thank Professor Louise Pape for critical reading of the manuscript and Professor Neville R. Kallenbach for helpful discussions.

REFERENCES

Antao, V. P., & Tinoco, I., Jr. (1992) *Nucleic Acids Res. 20*, 819–824.

Antao, V. P., Lai, S. Y., & Tinoco, I., Jr. (1991) *Nucleic Acids Res. 19*, 5901–5905.

Amaratunga, M., Pancoska, P., Paner, T. M., & Benight, A. S. (1989) *Nucleic Acids Res. 18*, 577–582.

Amaratunga, M., Snowden-Ifft, E., Wemmer, D. E., & Benight, A. S. (1992) *Biopolymers 32*, 865–879.

Ashley, G. W., & Kushlan, D. M. (1991) *Biochemistry 30*, 2927–2933.

Benight, A. S., Wang, Y. W., Amaratunga, M., Chattopadhyaya, R., Henderson, J., Hanlon, S., & Ikuta, S. (1989) *Biochemistry 28*, 3323–3332.

Berman, H. M., Neidle, S., Zimmer, C., & Thrum, H. (1979) *Biochim. Biophys. Acta 561*, 124–131.

Breslauer, K. J., Frank, R., Blocker, H., & Marky, L. A. (1986) *Proc. natl. Acad. Sci. U.S.A. 83*, 3746–3750.

Breslauer, K. J., Ferrante, R., Marky, L. A., Dervan, P. B., & Youngquist, R. S. (1988) *Structure & Expression Volume 2: DNA & Its Drug Complexes* (Sarma, M. H., & Sarma, R. H., Eds.) pp 273–290, Adenine Press, New York.

Cantor, C. R., Warshow, M. M., & Shapiro, H. (1970) *Biopolymers 9*, 1059–1077.

Caruthers, M. H. (1982) in *Chemical and Enzymatic Synthesis of Genme Fragments* (Gassen, H. G., & Lang, A., Eds.) pp 71–79, Verlag Chemie, Weinheim, FRG.

Chastain, M., & Tinoco, I., Jr. (1991) *Prog. Nucleic Acids Res. Mol. Biol. 41*, 131–177.

Chattopadhyaya, R., Ikuta, S., Grzewskowiak, K., & Dickerson, R. E. (1988) *Nature (London) 334*, 175–179.

Coll, M., Aymami, J., van der Marel, G. A., van Boom, J. H., Rich, A., & Wang, A. H. (1989) *Biochemistry 28*, 310–320.

Crothers, D. M. (1971) *Biopolymers 10*, 2147–2160.

Dervan, P. B. (1986) *Science (Washington, D.C.) 232*, 464–471.

Doktycz, M. J., Goldstein, R. F., Paner, T. M., Gallo, F., & Benight, A. S. (1992) *Biopolymers 32*, 849–864.

Draper, D. E. (1992) *Acc. Chem. Res. 25*, 201–207.

Erie, D. A., Sinha, N., Olson, W., Jones, R., & Breslauer, K. J. (1987) *Biochemistry 26*, 7150–7159.

Erie, D. A., Jones, R. A., Olson, W. K., Sinha, N. K., & Breslauer, K. J. (1989) *Biochemistry 28*, 268–273.

Freier, S. M., Kierzek, R., Jaeger, J. A., Sugimoto, N., Caruthers, M. H., Neilson, T., & Turner, D. H. (1986) *Proc. Natl. Acad. Sci. U.S.A. 83*, 9373–9377.

Garcia, A. E., Gupta, G., Sarma, M. H., & Sarma, R. H. (1988) *J. Biomol. Struct. Dyn. 6*, 525–542.

Garcia, A. E., Gupta, G., Soumpasis, D. M., & Tung, C. S. (1990) *J. Biomol. Struct. Dyn. 8*, 173–186.

Gralla, J., & Crothers, D. M. (1973) *J. Mol. Biol. 73*, 497–511.

Gupta, G., Sarma, M. H., Sarma, R. H., Bald, R., Engelke, U., Oei, S. L., Gessner, R., & Erdmann, V. A. (1987) *Biochemistry 27*, 7715–7723.

Haasnoot, C. A. G., Hilbers, C. W., van der Marel, G. A., van Boom, J. H., Singh, U. C., Pattabiraman, N., & Kollman, P. A. (1986) *J. Biomol. Struct. Dyn. 3*, 843–857.

Hahn, F. E. (1975) in *Antibiotics III: Mechanism of Action of Antimicrobial and Antitumor Agents* (Corcoran, J. W., & Hahn, F. E., Eds.) pp 79–100, Springer, New York.

Hare, D. R., & Reid, B. R. (1986) *Biochemistry 25*, 5341–5350.

Heus, H. A., & Pardi, A. (1991) *Science (Washington, D.C.) 253*, 191–194.

Hilbers, C. W., Hasnoot, C. A. G., de Bruin, S. H., Joorden, J. J., van der Marel, G. A., & van Boom, J. H. (1985) *Biochimie 67*, 685–695.

Hilbers, C. W., Blommers, M. J. J., van de Ven, F. J. M., van Boom, J. H., & van de Marel, G. A. (1991) *Nucleosides Nucleotides 10*, 61–80.

Ikuta, S., Chattopadhyaya, R., Dickerson, R. E., & Kearns, D. R. (1986) *Biochemistry 25*, 4840–4849.

Kopka, M. L., Yoon, C., Goodsell, D., Pjura, P., & Dickerson, R. E. (1985) *Proc. Natl. Acad. Sci. U.S.A. 82*, 1376–1380.

Luck, G., Triebel, H., Waring, M., & Zimmer, C. (1974) *Nucleic Acids Res. 1*, 503–530.

Maniatis, T., Ptashne, M., Backman, K., Kleid, D., Flashman, S., Jeffrey, A., & Maurer, R. (1975) *Cell 5*, 109–113.

Manning, G. S. (1978) *Q. Rev. Biophys. 11*, 179–246.

Marky, L. A. (1986) *Polymer Preprints 27*, 417–418.

Marky, L. A. (1990) *Biophys. J. 57*, 222a.

Marky, L. A., & Breslauer, K. J. (1987) *Biopolymers 26*, 1601–1620.

Marky, L. A., & Breslauer, K. J. (1987) *Proc. Natl. Acad. Sci. U.S.A. 84*, 4359–4363.

Marky, L. A., & Kupke, K. J. (1989) *Biochemistry 28*, 9982–9988.

Marky, L. A., Blumenfeld, K. S., Kozlowski, S., & Breslauer, K. J. (1983a) *Biopolymers 22*, 1247–1257.

Marky, L. A., Blumenfeld, K. S., & Breslauer, K. J. (1983b) *Nucleic Acids Res. 11*, 2857–2870.

Marky, L. A., Curry, J., & Breslauer, K. J. (1985) in *Molecular Basis of Cancer, Part B: Macromolecular Recognition, Chemotherapy and Immunology* (Rein, R., Ed.) pp 155–173, Alan R. Liss, Inc., New York.

Muller, U. R., & Fitch, W. M. (1982) *Nature (London) 298*, 582–585.

Panayotatos, N., & Wells, R. D. (1981) *Nature (London) 289*, 466–470).

Paner, T. M., Amaratunga, M., Doktycz, M. J., & Benight, A. S. (1990) *Biopolymers 29*, 1715–1731.

Patel, D. J. (1979) *Eur. J. Biochem. 99*, 369–378.

Patel, D. J. (1982) *Proc. Natl. Acad. Sci. U.S.A. 79*, 6424–6428.

Patel, D. J., & Canuel, L. L. (1977) *Proc. Natl. Acad. Sci. U.S.A. 74*, 5207–5211.

Pelton, J. G., & Wemmer, D. E. (1989) *Proc. Natl. Acad. Sci. U.S.A. 86*, 5723–5727.

Pelton, J. G., & Wemmer, D. E. (1990) *J. Am. Chem. Soc. 112*, 1393–1399.

Record, M. T., Jr., Anderson, C. F., & Lohman, T. M. (1978) *Q. Rev. Biophys. 11*, 103–178.

Rentzeperis, D., Kharakoz, D. P., & Marky, L. A. (1991) *Biochemistry 30*, 6276–6283.

Rosenberg, M., & Court, D. (1979) *Annu. Rev. Genet. 13*, 319–351.

Senior, M. M., Jones, R. A., & Breslauer, K. J. (1988) *Proc. Natl. Acad. Sci. U.S.A. 85*, 6242–6246.

Snowden-Ifft, E. A., & Wemmer, D. E. (1990) *Biochemistry 29*, 6017–6025.

Summers, M. F., Byrd, R. A., Gallo, K. A., Samson, C. J., Zon, G., & Egan, W. (1985) *Nucleic Acids Res. 13*, 6375–6393.

Taylor, J. S., Shultz, P. G., & Dervan, P. B. (1984) *Tetrahedron 40*, 457–465.

Unlenbeck, O. C. (1987) *Nature (London) 328*, 596–600.

Unlenbeck, O. C., Borer, P. N., Dengler, B., & Tinoco, I. (1973) *J. Mol. Biol. 73*, 483–496.

Varani, G., & Tinoco, I., Jr. (1991) *Q. Rev. Biophys. 24*, 279–532.

Ward, B., Rehfuss, R., Goodisman, J., & Dabrowiak, J. C. (1988) *Biochemistry 27*, 1198–1205.

Wartell, R. M., Larson, J. E., & Wells, R. D. (1974) *J. Biol. Chem. 249*, 6719–6732.

Wells, R. D., Goodman, T. C., Hillen, W., Horn, G. T., Klein, R. D., Larson, J. E., Muller, U. R., Neuendorf, S. K.,

Panayotatos, N., & Stirdivant, S. M. (1980) *Prog. Nucleic Acids Res. Mol. Biol. 25*, 167–267.

Wemmer, D. E., & Benight, A. S. (1985) *Nucleic Acids Res. 13*, 8611–8620.

Wemmer, D. E., Chou, S. H., Hare, D. R., & Reid, B. R. (1985) *Nucleic Acids Res. 13*, 3755–3772.

Wiseman, T., Williston, S., Brandts, J. F., & Lin, L. N. (1989) *Anal. Biochem. 179*, 131–137.

Williamson, J. R., & Boxer, S. G. (1989a) *Biochemistry 28*, 2819–2831.

Williamson, J. R., & Boxer, S. G. (1989b) *Biochemistry 28*, 2831–2836.

Wolk, S., Hardin, C. C., Germann, M. W., van de Sande, J. H., & Tinoco, I., Jr. (1988) *Biochemistry 27*, 6960–6967.

Xodo, L. E., Manzini, G., Quadrifoglio, F., van der Marel, G. A., & van Boom, J. H. (1986) *Nucleic Acids Res. 14*, 5389–5398.

Xodo, L. E., Manzini, G., Quadrifoglio, F., van der Marel, G. A., & van Boom, J. H. (1988a) *Biochemistry 27*, 6321–6326.

Xodo, L. E., Manzini, G., Quadrifoglio, F., van der Marel, G. A., & van Boom, J. H. (1988b) *Biochemistry 27*, 6327–6331.

Zieba, K., Chu, T. M., Kupke, D. W., & Marky, L. A. (1991) *Biochemistry 30*, 8018–8026.

Zimmer, C., & Wahnert, U. (1986) *Prog. Biophys. Mol. Biol. 47*, 31–112.